Electronic Supplementary Material (ESI) for Lab on a Chip.

A Microsystem Integrating Photodegradable Hydrogel Microstructures and Reconfigurable Microfluidics for Single Cell Analysis and Retrieval

Kyung Jin Son, Dong-Sik Shin, Timothy Kwa, Jungmok You, Yandong Gao and Alexander Revzin

Supporting information

E-mail: arevzin@ucdavis.edu

Preparation of an array of photodegradable hydrogel islands and selective cell release

The oxygen plasma chamber (YES-R3, San Jose, CA, USA) was used to clean the glass substrates (75 × 25 mm^2, Fisher Scientific) at 300 W for 15 min. The cleaned glass substrates were incubated in 0.1% (v/v) 3-acryloypropyl trichlorosilane (Gelest, USA) in anhydrous toluene (Sigma Aldrich, USA) for 1 h under nitrogen purge to generate acrylates on glass surfaces. The glass slides were rinsed with fresh toluene, dried under nitrogen, and cured at 100°C for 2 h. The generated acryl silane-modified substrates were used immediately or placed in a desiccator until future use.

Our photodegradable hydrogels consist of poly(ethylene glycol) (PEG) and a photolabile linker (PLL) containing light sensitive *o*-nitrobenzyl groups. Previously, our laboratory reported a novel photolabile crosslinker (PCL) synthesis route and demonstrated its application for sorting and selective retrieval of microbeads as well as cells[1]. The synthesized photolabile crosslinker

was grafted with the methacryl groups at both ends, resulting in PEG-PLL-diacrylates (PEG-PLL-DA) as described in the previous report[1, 2]. In this paper, photodegradable hydrogels were prepared via chemically initiated polymerization of PEG-PLL-DA and acrylated NeutrAvidin (Acryl-NAv). A solution of NeutrAvidin (1mg mL^{-1} in PBS; Thermo Scientific, USA) was reacted with 10 mg mL^{-1} of Acrylic poly(ethylene glycol) N-hydroxysulfosuccinimide (Acryl-PEG-NHS, MW 3.4k, Laysan Bio) in the presence of 0.1 M $NaHCO_3$ (Sigma Aldrich) for overnight at 4°C to prepare the acrylated NeutrAvidin. Monomer solution for functional photodegradable hydrogel were prepared by dissolving 10% (w/v) PEG-PLL-DA, 40% (v/v) Acryl-NAv, 5% (v/v) Poly(ethylene glycol) monoacrylate) (PEG-A, Sigma Aldrich), 0.025M Ammonium persulfate (AP, Sigma Aldrich), and 0.025 M tetramethylethylenediamine (TEMED, Sigma Aldrich) in PBS. Monomer solutions were loaded onto the silane-treated glass, covered with a cover glass (24×30×0.13 mm, Fisher Scientific), and incubated for 2 h at RT or overnight at 4°C to form a uniform layer of NAv-modified photodegradable hydrogels.

The slides with a uniform layer of NAv-modified photodegradable hydrogels were irradiated through the photomask from an illuminator for 9.5 sec by a 365 nm UV light source (500 mW cm^{-2}; OmniCure Series 1000, Lumen Dynamics Group, Canada), and incubated with PBS for overnight at 4°C to degrade the hydrogel selectively and remove the degraded hydrogel from substrates. To capture the single cells on the generated photogel islands (diameter = 20 μm), the slides were further incubated with biotinylated CD4 antibodies (0.2 mg mL^{-1} in PBS; Beckman Coulter, Inc.) for 2 h at RT, washed with DI water, and dried under nitrogen.

For selective retrieval of single cells after measurement, photodegradable hydrogel islands capturing single cells were exposed to 405 nm UV from a fluorescence microscope (45 mW cm^{-2}, exposure diameter = 40 μm; Nikon Instruments, Inc.). After incubation for 1 h at 37°C,

the exposed cell capture islands were degraded, and specific single cells detached from the surface.

Fabrication of reconfigurable microfluidic device

A PDMS reconfigurable microfluidic device with a reversibly collapsible micropatterned layer was employed to augment sensitivity and inhibit cross-talk between neighboring microchambers. The device which consists of a bottom flow layer (thickness = 400 μm) containing 558 microchambers and a top control layer (thickness = 1 cm) was prepared via a multilayer soft lithography method reported previously[3]. A solution of PDMS (Sylgard 184, Dow Corning) was mixed with curing agent at a 10: 1 curing ratio, and placed onto a photoresist (SU-8 2025, Microchem) patterned substrate. After removing air bubbles under vacuum, the flow layer was baked for 20 minutes and the control layer was baked for 25 minutes at 70°C. A hole was punched in the control layer to apply and release vacuum into control layer, and then two layers were aligned carefully by eye. The device with adhered two layers was fully cured by baking for 1 h and cut out from substrate, and holes were punched for vacuum web, inlet and outlet. Consequently, the reconfigurable microfluidic device was aligned with existing photodegradable hydrogels with fiduciary marks, and used for experiments.

Cell culture condition

U-937 cells were purchased from American Type Culture Collection (ATCC) and cultured in RPMI-1640 media (Life Technologies, USA) supplemented with 10% (v/v) fetal bovine serum (FBS, Invitrogen, USA), 100 U mL^{-1} penicillin, and 100 μg mL^{-1} streptomycin at 37°C in a humidified 5% CO_2 atmosphere.

For experiment, the culture media was removed via centrifugation and the cells were resuspended in serum-free and Phenol Red-free RPMI-1640 media. To monitor protease secretion, U-937 cells were mitogenically activated with 100 ng mL^{-1} of phorbol 12-myristate 13-acetate (PMA, Sigma Aldrich). A cell culture chamber was built on a Nikon eclipse Ti fluorescence microscope (Nikon Instruments, Inc.) for live-cell analysis, maintaining the environmental conditions for optimal growth and functioning of cells during experiment. The temperature of our device was controlled by Tokai Hit Thermo-E microscope heating stage (Tokai Hit, Japan) while 5% CO_2 was supplied to the incubator.

Computational modeling of peptide cleavage

We assumed that the enzymatic activity of MMP9 follows Michaelis – Menten kinetics. When MMP9 molecules (E) secreted from cell encounter free floating FRET peptides (S) in solution, MMP9 catalyzes and cleaves FRET peptides to FITC-containing peptides (P; Met-Trp-Ser-Arg-Glu-Cys) and DABCYL-containing fragments by the following pathway.

$$E + S \underset{k_{-1}}{\overset{k_1}{\rightleftarrows}} ES \xrightarrow{k_{cat}} E + P$$

The rate of this homogeneous proteolytic reaction is simply given by the following Michaelis – Menten equation on the assumption that concentration of the complex ES, [*ES*], is relatively negligible compared to [P] and $[S]_0$:

$$\frac{d[P]}{dt} = \frac{k_{cat}[E]([S]_0 - [P])}{K_m + ([S]_0 - [P])} \quad (1)$$

where $[S]_0$ is the initial concentration of free floating FRET peptides in solution and K_m is the Michaelis – Menten constant which is defined as $(k_{cat} + k_{-1}) / k_1$. To study real-time enzyme kinetics, we employed the following Schnell-Mendoza equation[4] as a solution for the equation (1):

$$\frac{[P]}{[S]_0} = 1 - \frac{K_m}{[S]_0} W\left(\frac{[S]_0}{K_m} \exp\left(\frac{-k_{cat}[E]t + [S]_0}{K_m}\right)\right) \quad (2)$$

where W is the Lambert-W function satisfying the transcendental equation.

On the assumption that $[P]/[S]_0$ is linearly related to the fluorescence signal, K_m and k_{cat} were estimated by matching equation (2) to the experimental data from Figure 2A using non-linear least squares fitting ("nlinfit" routine) function and Lambert W function ("lambertw") in MATLAB (MathWorks Inc., USA).

Real-time monitoring of MMP9 secretion from U-937 single cells

The fluorescence signals of free floating sensing peptides in microchambers were monitored after the flow layer of reconfigurable microfluidic device was collapsed. Time-lapse images of device were acquired at 10 min intervals for a total of 120 min as shown in Fig. S1 and S2. Dramatic increase in fluorescence was detected from microchambers having activated single cells while only slight increase in fluorescence was observed from quiescent single cells. The fluorescence intensities achieved from mitogenically activated U-937 single cells (Fig. S1) and quiescent single cells (Fig. S2) was quantitatively analyzed by percent fluorescence increase in Fig. 3C. We also monitored the sensing peptides in microchambers not having cells but only negligible increase in fluorescence was observed.

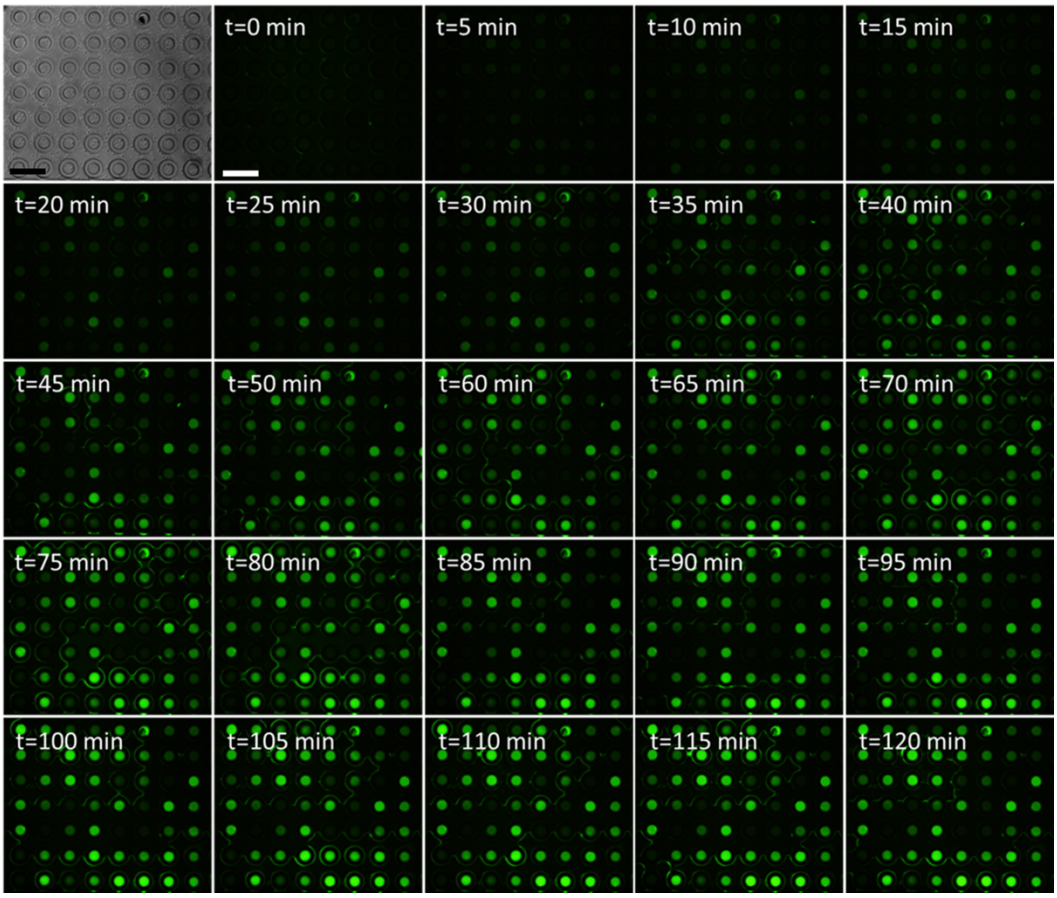

Figure S1. Time-lapse images showing fluorescence change of FRET peptides in microwells with activated U-937 cells. Scale bar = 150 μm.

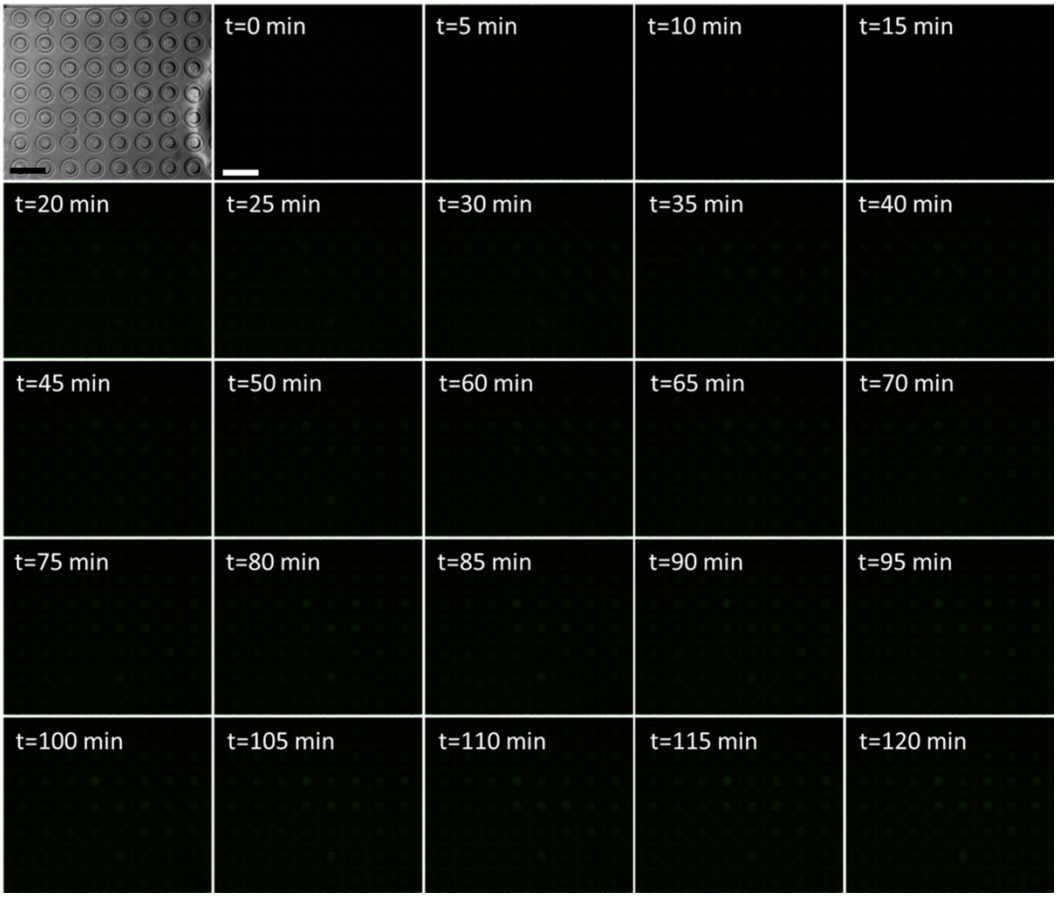

Figure S2. Time-lapse images showing fluorescence change of FRET peptides in microwells with quiescent U-937 cells. Scale bar = 150 μm.

Viability/Cytotoxicity test

The viability of U-937 cells residing on Ab functionalized photogel during measurement was determined using LIVE/DEAD assay (Molecular Probes, Eugene, OR). Figure S5 demonstrates that cell viability was excellent, ranging from 99.8 ± 0.1% at the beginning to 96.5 ± 1.4% at the end of the experiment. This suggests that heterogeneity in MMP production/activity may not be due to cell death but is more likely due to intrinsic differences in cellular functionality.

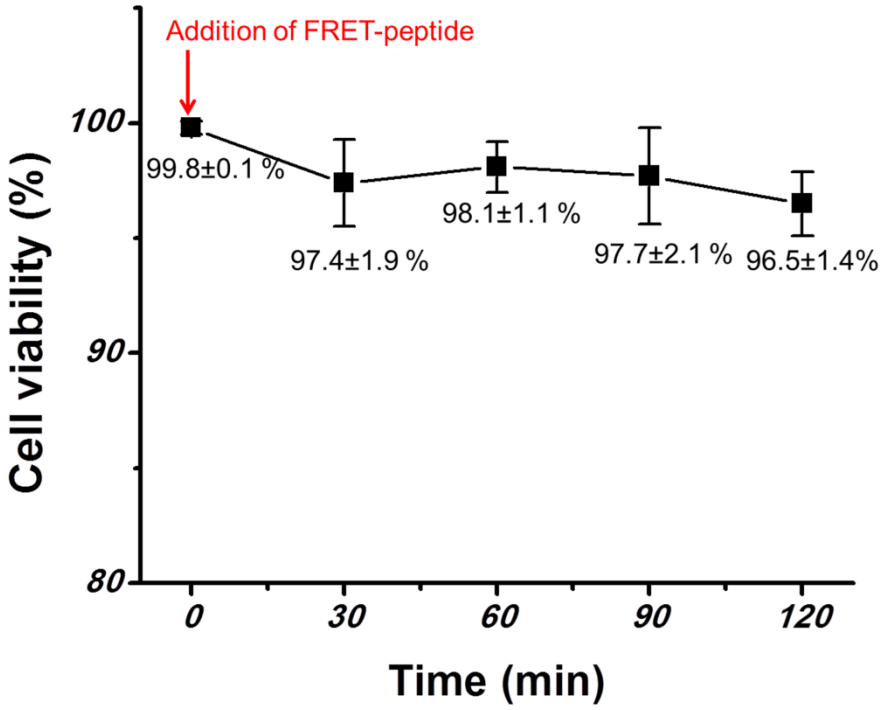

Figure S3. Cell viability during measurement.

Numerical simulation for quantification of MMP9 secretion from single cell

To quantify MMP9 secreted from activated U-937 single cells and determine the MMP9 secretion rate (R_{sec}), the reaction – diffusion model was applied to the experimental data in Fig. 3A using COMSOL Multiphysics (COMSOL, Inc., Burlington, MA). Inside the microchambers, MMP9 molecules secreted from captured single cell diffuse and react with soluble, free floating FRET-peptides (S). The homogeneous reaction – diffusion equations for MMP9 (E) and FITC-containing cleaved peptides (P) in solution can be described as[5]:

$$\frac{\partial[E]}{\partial t} = D_E \nabla^2[E] \tag{3}$$

$$\frac{\partial[P]}{\partial t} = D_P \nabla^2[P] + k_{cat}[ES] \tag{4}$$

where D_E and D_P are the diffusion coefficients of MMP9 and FITC-containing cleaved peptides in solution. Diffusivity of MMP9 in solution (D_E; MW = 92,000) was taken to be 8.18×10^{-7} cm^2 s^{-1},[6] and that of FITC-containing cleaved peptides (D_P; MW = 1169.25) was determined to be 4.07×10^{-6} cm^2 s^{-1} based on the previous literature[7]. In Equation (4), the concentration of complex, [ES], can be replaced by $\frac{[E]([S]_0 - [P])}{K_m + ([S]_0 - [P])}$ on the assumption of Michaelis – Menten kinetics.

MMP9 production of U-937 single cells was simulated based on the cylindrical geometry of microchambers (radius = 30 μm, height = 50 μm). On the assumption of MMP9 secretion rate R_{sec}, [P] can be numerically calculated, resulting in theoretical signal which is linearly related to $[P]/[S]_0$ inside the microchamber. Here, we assumed that cells secrete MMP9 from the beginning of measurement with constant secretion rate, R_{sec}. By matching generated theoretical signal to experimental data, MMP9 secretion rate was determined iteratively with ~10% of root mean square (RMS) deviations. Subsequently, concentrations profiles of MMP9 (E), FRET-peptides (S), and cleaved peptides (P) were achieved for activated single cells (Fig. 3E) and quiescent single cells (Fig. S5).

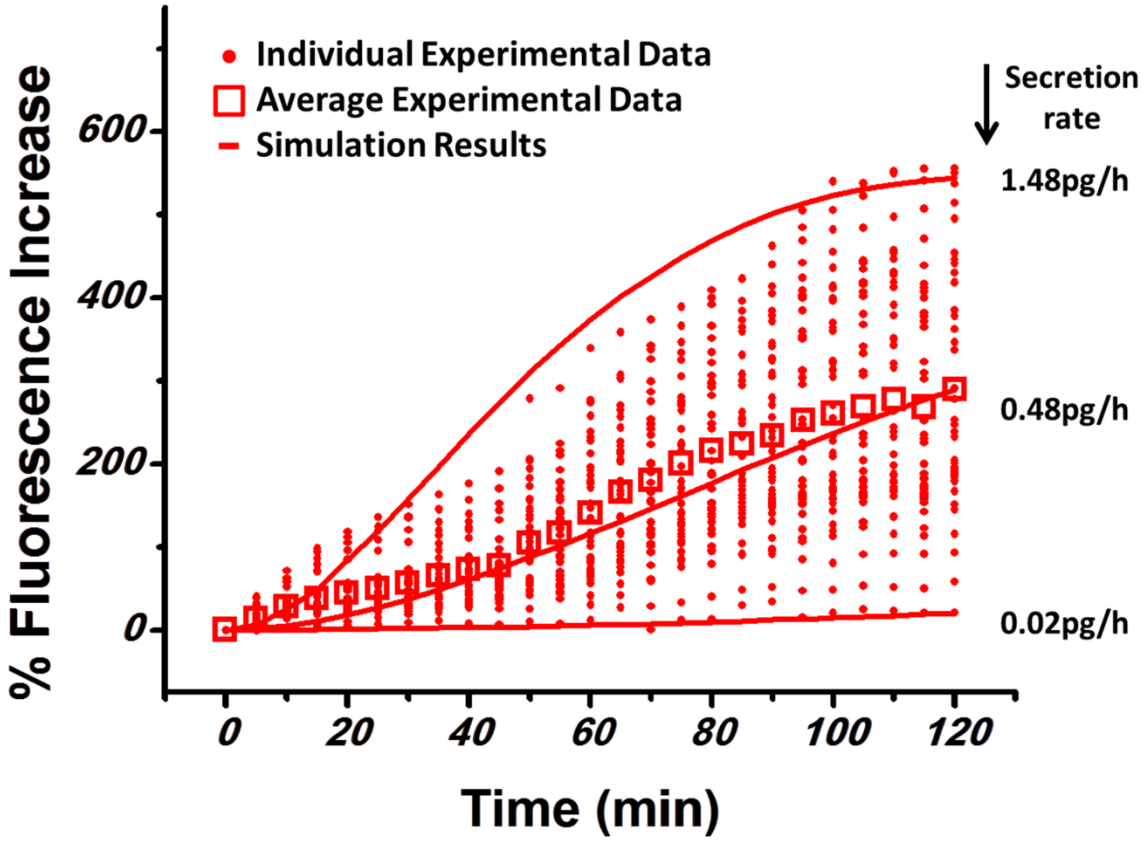

Figure S4. Comparison of simulation results (solid lines) with experimental data (individual data: dots, average: squares) showing change in fluorescence increase over time for activated single cells. MMP9 secretion rates are 0.48 pg h^{-1} for single cells at average secretion level, 1.48 pg h^{-1} for highest MMP9 expressing single cells and 0.02 pg h^{-1} for lowest MMP9 expressing single cells. RMS deviations: 9.8 % for average MMP9 expressing, 8.2% for highest expressing, 7.5% for lowest expressing single cells.

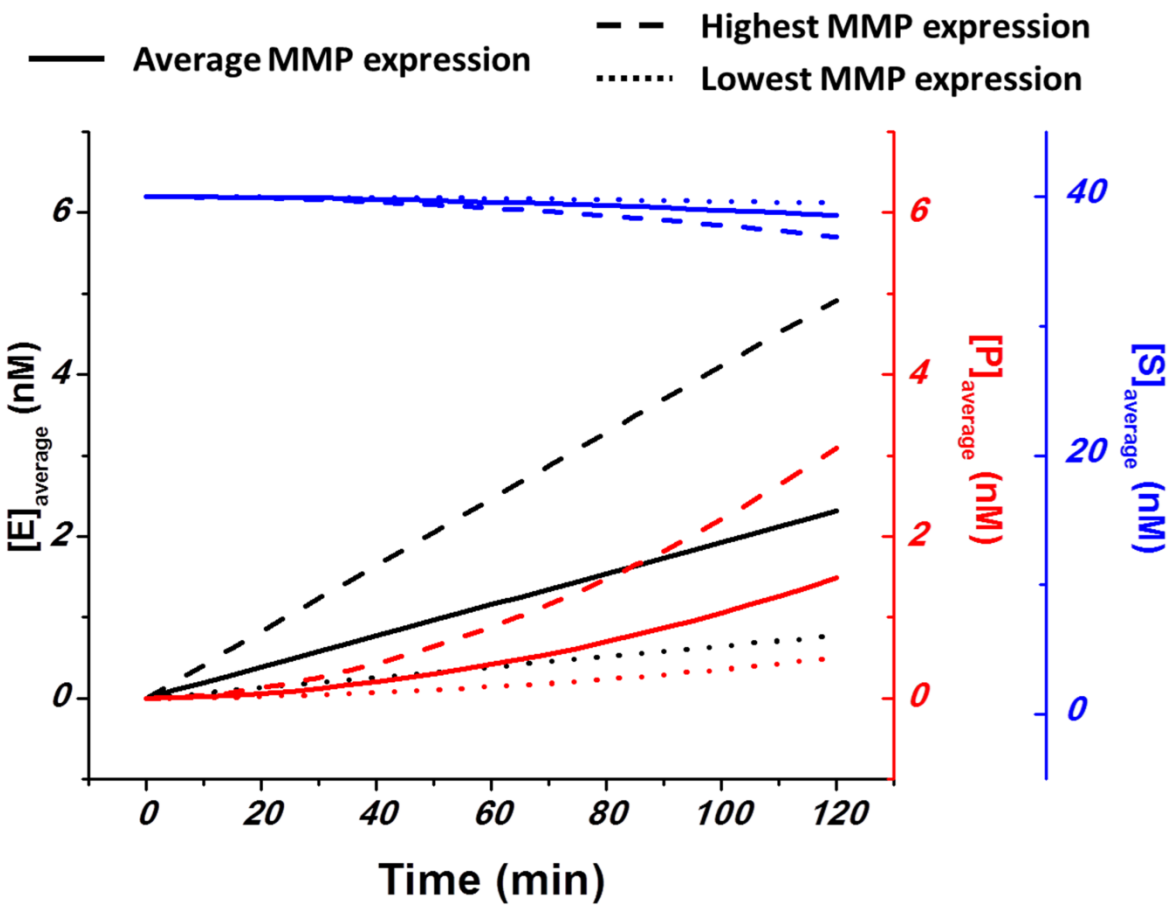

Figure S5. Numerical simulation results showing the average concentration profile of MMP9, FRET-peptides, and cleaved peptides over time for quiescent single cells.

1. C. Siltanen, D. S. Shin, J. Sutcliffe and A. Revzin, *Angew Chem Int Edit*, 2013, **52**, 9224-9228.
2. D. S. Shin, J. You, A. Rahimian, T. Vu, C. Siltanen, A. Ehsanipour, G. Stybayeva, J. Sutcliffe and A. Revzin, *Angewandte Chemie*, 2014.
3. M. A. Unger, H. P. Chou, T. Thorsen, A. Scherer and S. R. Quake, *Science*, 2000, **288**, 113-116.
4. S. Schnell and C. Mendoza, *J Theor Biol*, 1997, **187**, 207-212.
5. A. R. Tzafriri, M. Bercovier and H. Parnas, *Biophysical journal*, 2002, **83**, 776-793.
6. M. T. Tyn and T. W. Gusek, *Biotechnology and bioengineering*, 1990, **35**, 327-338.

7. O. Hosoya, S. Chono, Y. Saso, K. Juni, K. Morimoto and T. Seki, *The Journal of pharmacy and pharmacology*, 2004, **56**, 1501-1507.